

A series test of the scaling limit of self-avoiding walks

Anthony J. Guttmann¹

*ARC Centre of Excellence for
Mathematics and Statistics of Complex Systems,
Department of Mathematics and Statistics,
The University of Melbourne, Victoria 3010, Australia*

Jesper L. Jacobsen²

*LPTENS, École Normale Supérieure, 24 rue Lhomond, 75231 Paris, France
Université Pierre et Marie Curie, 4 place Jussieu, 75252 Paris, France*

Abstract

It is widely believed that the scaling limit of self-avoiding walks (SAWs) at the critical temperature is (i) conformally invariant, and (ii) describable by Schramm-Loewner Evolution (SLE) with parameter $\kappa = 8/3$. We consider SAWs in a rectangle, which originate at its centre and end when they reach the boundary. We assume that the scaling limit of SAWs is describable by SLE_κ , with the value of κ to be determined. It has previously been shown by Guttmann and Kennedy [11] that, in the scaling limit, the ratio of the probability that a SAW hits the side of the rectangle to the probability that it hits the end of the rectangle, depends on κ . By considering rectangles of fixed aspect ratio 2, and also rectangles of aspect ratio 10, we calculate the probabilities exactly for larger and larger rectangles. By extrapolating this data to infinite rectangle size, we obtain the estimate $\kappa = 2.66664 \pm 0.00007$ for rectangles of aspect ratio 2 and $\kappa = 2.66675 \pm 0.00015$ for rectangles of aspect ratio 10. We also provide numerical evidence supporting the conjectured distribution of SAWs striking the boundary at various points in the case of rectangles with aspect ratio 2.

1 Introduction

A self-avoiding walk (SAW) of length n on a periodic graph or lattice \mathcal{L} is a sequence of distinct vertices w_0, w_1, \dots, w_n in \mathcal{L} such that each vertex is a nearest neighbour of its predecessor. In Figure 1 a very long walk of 2^{25} steps is shown (generated by a Monte Carlo algorithm [4]).

Consider now those SAWs starting at the centre of an $L \times W$ rectangle and ending when they hit the boundary. We take the scaling limit of SAW, at the critical point, in the usual

¹email: tonyg@ms.unimelb.edu.au

²email: jesper.jacobsen@ens.fr

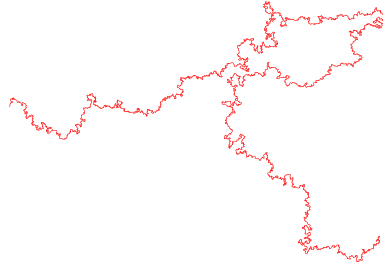


Figure 1: A typical two-dimensional SAW of 2^{25} steps on the square lattice – courtesy of Nathan Clisby.

way (described, for example, in [11]). Let p_L be the probability that a randomly chosen SAW, in the scaling limit, hits the side of the rectangle before the end, and let $p_W = 1 - p_L$ be the probability that it hits the end before the side. In Guttman and Kennedy [11] the probability ratio p_L/p_W was calculated, under the assumption that the scaling limit is describable by $\text{SLE}_{8/3}$. For a rectangle of aspect ratio $r = L/W$, with parameter b , where $b = \frac{3}{\kappa} - \frac{1}{2}$, they found, asymptotically,

$$\frac{p_W}{p_L} = \frac{2^{2b+1}\Lambda}{b} e^{-b\pi r/2} \left[1 + \frac{\Lambda 2^{b+1}}{b \sin\left(\frac{\pi b}{2}\right)} e^{-b\pi r/2} + 4(b-1+2\Lambda) e^{-\pi r/2} + O(e^{-b\pi r}) \right],$$

for $0 < b < 1$, where $\Lambda = \left(\frac{\Gamma(\frac{1+b}{2})}{\Gamma(\frac{b}{2})} \right)^2$. The exact result is given as the ratio of two integrals (5), and we give an outline of their calculation in the following section.

In this work, we have considered all $2n \times 4n$ rectangles of aspect ratio 2 of size 2×4 up to 18×36 , and have generated all SAW starting at the origin and ending on the boundary of the rectangles. We have also considered all $2n \times 20n$ rectangles of aspect ratio 10 of size 2×20 up to 14×140 . We have also developed a refined enumeration scheme in which the full hitting distribution is recorded; we give the results here for rectangles of aspect ratio 2. The relevant geometry is shown in Figure 3. We obtained separately the generating functions for SAWs starting at the centre of the rectangle and exiting at any prescribed point on its boundary. This has been compared to that calculated by conformal mapping, assuming that $\text{SLE}_{8/3}$ is the appropriate scaling limit.

The data was generated using a transfer matrix formalism, utilising symmetry and similar techniques to minimise the computational complexity. Details of the methods used are given in Section 2. In addition to the position of the end-points of the walks on the boundary, the length (number of steps) was also retained.

In [12] a Monte Carlo study was made by Kennedy, who compared certain random variables associated with SAWs in a half-plane with those predicted assuming that the scaling limit of SAWs is given by $\text{SLE}_{8/3}$. Excellent agreement was found in a visual comparison of two graphical plots. Our work differs in nature in that we predict a specific value of κ , assuming that the scaling limit of SAWs is given by SLE_{κ} .

1.1 Conformal mapping

Let D be a bounded, simply connected domain in the complex plane containing 0. We are interested in paths in D starting at 0 and ending on the boundary of the domain. Initially we will consider random walks, later self-avoiding walks. We can discretize the space with a lattice of lattice spacing δ . In both the random walk case and the SAW case we are then interested in the scaling limit $\delta \rightarrow 0$. For random walks the scaling limit is Brownian motion, stopping when it hits the boundary of D . The distribution of the end-point is harmonic measure. If the domain boundary is piecewise smooth, then harmonic measure is absolutely continuous with respect to arc length along the boundary [19]. Let $h_D(z)$ denote the density with respect to arc length (often called the Poisson kernel). If f is a conformal map on D that fixes the origin, and such that the boundary of $f(D)$ is also piecewise smooth, then the conformal invariance of Brownian motion implies that the density for harmonic measure on the boundary of $f(D)$ is related to the boundary of D by

$$h_D(z) = |f'(z)| h_{f(D)}(f(z)). \quad (1)$$

In the case of the SAW, Lawler, Schramm, and Werner [15] predicted that the corresponding density of the probability measure $\rho(z)$ transforms under conformal maps as

$$\rho_D(z) = c |f'(z)|^b \rho_{f(D)}(f(z)), \quad (2)$$

where $b = 5/8$ and the constant c is required to ensure that $\rho_D(z)$ is a probability density. If one starts the random walk or the SAW at the centre of a disc, then the hitting density on the circle will be uniform. So the above equations determine the hitting density for any simply connected domain, by virtue of the Riemann mapping theorem. Simulations in [7], [14] and [13] provide strong support for the conjectured behaviour. (Eq. (2) is correct for domains whose boundary consists only of vertical and horizontal line segments. For general domains there is a lattice effect that persists in the scaling limit that produces a factor that depends on the angle of the tangent to the boundary that must be included [14].)

The solution of the problem for random walks by conformal maps is described in [2], where a conformal map from the unit disc to an $a \times c$ rectangle is given by the Schwarz-Christoffel formula. Our approach also uses conformal maps, but we instead use a map between the upper half-plane and a rectangle, where the mapping is again given by a Schwarz-Christoffel transformation. For $\alpha > 1$, let

$$f(z) = \int_0^z \frac{d\xi}{\sqrt{1-\xi^2}\sqrt{\alpha^2-\xi^2}}.$$

$f(z)$ is a Schwarz-Christoffel transformation that maps the upper half plane to a rectangle. The rectangle has one edge along the real axis and 0 is a midpoint of this side. So the corners can be written as $\pm a/2$ and $ic \pm a/2$ where $a, c > 0$ are the length of the horizontal and vertical edges, respectively. We have

$$f(1) = a/2, \quad f(-1) = -a/2, \quad f(\alpha) = a/2 + ic, \quad f(-\alpha) = -a/2 + ic, \quad f(0) = 0.$$

So

$$a = \int_{-1}^1 \frac{dx}{\sqrt{1-x^2}\sqrt{\alpha^2-x^2}}, \quad c = \int_1^\alpha \frac{dx}{\sqrt{x^2-1}\sqrt{\alpha^2-x^2}}.$$

We note that

$$a = \frac{2}{\alpha} \mathbf{K} \left(\frac{1}{\alpha} \right), \quad c = \frac{1}{\alpha} \mathbf{K} \left(\frac{\sqrt{\alpha^2 - 1}}{\alpha} \right), \quad \alpha > 1.$$

Here $\mathbf{K}(x)$ is the complete elliptic integral of the first kind. By dilation invariance we only need concern ourselves with the aspect ratio $r = a/c$. So given an aspect ratio r , we have to find α such that

$$r = \frac{\int_{-1}^1 (1-x^2)^{-1/2} (\alpha^2 - x^2)^{-1/2} dx}{\int_1^\alpha (x^2 - 1)^{-1/2} (\alpha^2 - x^2)^{-1/2} dx} = \frac{2\mathbf{K} \left(\frac{1}{\alpha} \right)}{\mathbf{K} \left(\frac{\sqrt{\alpha^2 - 1}}{\alpha} \right)}.$$

From the properties of elliptic integrals, it follows [11] that

$$\sqrt{\alpha} = \frac{\theta_3(e^{-2\pi/r})}{\theta_2(e^{-2\pi/r})}, \quad (3)$$

where $\theta_j(q) = \theta_j(0, q)$ is the Jacobi theta function. Evaluating this in one's favourite algebraic package gives the required value of α for any $r \geq 1$ instantly.

Alternatively, we note that for an aspect ratio of 10, α is very close to 1. We can achieve very high accuracy by expanding the ratio of the above integrals around $\alpha = 1$, and find

$$r = \frac{1}{\pi} \left(4 \log(2\sqrt{2}) - 2 \log(\alpha - 1) + (\alpha - 1) - \frac{3}{8}(\alpha - 1)^2 + \frac{5}{24}(\alpha - 1)^3 + O(\alpha - 1)^4 \right).$$

Solving this numerically for $r = 10$ gives $\alpha = 1.00000120561454706472212 \dots$. To leading order one obtains

$$\alpha \approx 1 + 8e^{-\pi r/2} + 32e^{-\pi r},$$

which for $r = 10$ gives 19 digit accuracy.

An alternative approach is to note that

$$r = \frac{2\mathbf{K}' \left(\frac{\sqrt{\alpha^2 - 1}}{\alpha} \right)}{\mathbf{K} \left(\frac{\sqrt{\alpha^2 - 1}}{\alpha} \right)},$$

so that when $r^2 = 0 \pmod{4}$, one has

$$\frac{\sqrt{\alpha^2 - 1}}{\alpha} = k_{r^2/4}.$$

Here k_n are *singular moduli*, that is, elliptic moduli for which $\frac{\mathbf{K}(k_n)}{\mathbf{K}'(k_n)} = \frac{1}{\sqrt{n}}$. From a table of singular moduli, for example [18], one finds for $r = 10$ that

$$\alpha = \frac{\sqrt{2 + 24\sqrt{161\sqrt{5} - 360}}}{1 + 12\sqrt{161\sqrt{5} - 360}}.$$

For aspect ratio $r = 2$, one finds $\alpha = \sqrt{2}$.

These considerations establish α , a parameter of the conformal map, both directly and asymptotically. To proceed further we need to determine the behaviour of the hitting density of paths from the origin to the boundary of the rectangle.

First, note that the preimage of the center of the rectangle will, by symmetry, be on the imaginary axis, so write it as di . In [11] geometrical arguments are given to show that $d = \sqrt{\alpha}$. An alternative algebraic derivation is the following: From the Schwarz-Christoffel mapping $f(z) = \int_0^z \frac{d\xi}{\sqrt{1-\xi^2}\sqrt{\alpha^2-\xi^2}}$, set $u = -i\xi$, giving $ic/2 = f(id) = i \int_0^d \frac{du}{\sqrt{1+u^2}\sqrt{\alpha^2+u^2}}$. This integral is an (incomplete) elliptic integral of the second kind, from which follows $d = \sqrt{\alpha}$.

As shown in [11], for both the random walk and the SAW in the half plane starting at id , the (unnormalized) hitting density along the real axis is $(x^2 + d^2)^{-b} = (x^2 + \alpha)^{-b}$. Hence the hitting density ρ_R for walks in a rectangle starting at the center is

$$(x^2 + \alpha)^{-b} \propto |f'(x)|^b \rho_R(f(z)). \quad (4)$$

The ratio of probabilities of a walk first hitting an end of the rectangle to that of a walk first hitting a side is just the ratio of the integral of the hitting density $\rho(z)$ along a vertical edge to the integral along a horizontal edge,

$$\frac{\int_0^c \rho_R(a/2 + iy) dy}{\int_{-a/2}^{a/2} \rho_R(x) dx}.$$

By a change of variable, setting $u = f^{-1}(x)$ in the denominator and $u = f^{-1}(a/2 + iy)$ in the numerator, and recalling that $f'(u) = (1 - u^2)^{-1/2}(\alpha^2 - u^2)^{-1/2}$, the ratio of probabilities of a first hit on the vertical side to a first hit on the horizontal side, $R(\alpha, b)$, is

$$R(\alpha, b) = \frac{\int_1^\alpha (u^2 + \alpha)^{-b} (u^2 - 1)^{(b-1)/2} (\alpha^2 - u^2)^{(b-1)/2} du}{\int_{-1}^1 (u^2 + \alpha)^{-b} (1 - u^2)^{(b-1)/2} (\alpha^2 - u^2)^{(b-1)/2} du}. \quad (5)$$

These integrals cannot be solved in closed form. Both Mathematica and Maple can be used to evaluate them numerically to any reasonable accuracy. However for our purposes it would be useful to have a reasonably accurate asymptotic representation.

We will calculate the leading order and first correction term in the quotient (5) where $b \in (0, 1]$ and $\alpha = 1 + c$, with $|c| \ll 1$. Here α is related to the aspect ratio r of a rectangle by (3). Consider the numerator first. One has

$$N(\alpha, b) = \int_1^\alpha (u^2 + \alpha)^{-b} (\alpha^2 - u^2)^{(b-1)/2} (u^2 - 1)^{(b-1)/2} du.$$

Now, since $u = 1 + \epsilon$ with $\epsilon \ll 1$,

$$\begin{aligned} (u^2 + \alpha) &\approx (2u + c), \\ (\alpha^2 - u^2) &= (\alpha - u)(\alpha + u) \approx (2 + c + (u - 1))(\alpha - u), \\ (u^2 - 1) &= (u + 1)(u - 1) = (2 + (u - 1))(u - 1). \end{aligned} \quad (6)$$

So

$$N(\alpha, b) \approx 2^{b-1} \cdot \left(1 + \frac{c(b-1)}{4}\right) \cdot \int_1^\alpha (2u + c)^{-b} (\alpha - u)^{\frac{b-1}{2}} (u - 1)^{\frac{b-1}{2}} du$$

$$+ 2^{b-2} \cdot \int_1^\alpha (2u+c)^{-b} (\alpha-u)^{\frac{b-1}{2}} (u-1)^{\frac{b+1}{2}} du.$$

Set $u = 1 + tc$. Then $du = c \cdot dt$, and

$$\begin{aligned} N(\alpha, b) &\approx \frac{c^b}{2} \left(1 + \frac{c(b-1)}{4}\right) \left(\int_0^1 \left(1 + \frac{b-1}{2}tc\right) [t(1-t)]^{\frac{b-1}{2}} dt - \frac{bc}{2} \cdot \int_0^1 (1+2t)[t(1-t)]^{\frac{b-1}{2}} dt \right) \\ &= \left(1 + \frac{c(b-1)}{4}\right) \left((\alpha-1)^b \frac{\sqrt{\pi} \cdot \Gamma(\frac{1}{2} + \frac{b}{2})}{2^{b+1} \cdot \Gamma(1 + \frac{b}{2})} (1 + \frac{b-1}{4}c) - (\alpha-1)^{b+1} \frac{b \cdot \sqrt{\pi} \cdot \Gamma(\frac{1}{2} + \frac{b}{2})}{2^{b+1} \cdot \Gamma(1 + \frac{b}{2})} \right) \\ &= (\alpha-1)^b \frac{\sqrt{\pi} \cdot \Gamma(\frac{1}{2} + \frac{b}{2})}{2^{b+1} \cdot \Gamma(1 + \frac{b}{2})} \left[1 - \frac{(b+1)}{2}(\alpha-1) \right]. \end{aligned} \quad (7)$$

Next, consider the denominator:

$$F(\alpha, b) = 2 \int_0^1 (\alpha + u^2)^{-b} [(1-u^2)(\alpha^2 - u^2)]^{(b-1)/2} du$$

Again, let $\alpha = 1 + c$, where $|c| \ll 1$. One has

$$(1 + c + x^2)^{-b} \approx (1 + x^2)^{-b} \left(1 - \frac{bc}{1 + x^2} \right),$$

and

$$(\alpha^2 - x^2) \approx (1 - x^2 + 2c),$$

both to first order in c . So with $t = 2c$, $F(\alpha, b) \approx 2(I(b, t) - bcI(b+1, t))$, where

$$I(b, t) = \int_0^1 (1 + x^2)^{-b} [(1 - x^2)(1 - x^2 + t)]^{(b-1)/2} dx.$$

(Note that the first argument refers to the power of $(1 + x^2)$ only, not the other occurrences of b). Next, we take the Mellin transform

$$\int_0^\infty \frac{t^{s-1}}{(1 - x^2 + t)^{(1-b)/2}} dt = B\left(s, \frac{1-b}{2} - s\right) (1 - x^2)^{s+(b-1)/2}.$$

So the Mellin transform of $I(b, t)$ is

$$\begin{aligned} B\left(s, \frac{1-b}{2} - s\right) \int_0^1 (1 + x^2)^{-b} (1 - x^2)^{b+s-1} dx = \\ \frac{\sqrt{\pi}}{2} B\left(s, \frac{1-b}{2} - s\right) \frac{\Gamma(b+s)}{\Gamma(\frac{1}{2} + b + s)} {}_2F_1\left(\frac{1}{2}, b; \frac{1}{2} + b + s; -1\right). \end{aligned}$$

Hence the inverse transform is

$$I(b, t) = \frac{\sqrt{\pi}}{2\Gamma(\frac{1-b}{2})} \int_{d-i\infty}^{d+i\infty} \frac{ds}{2\pi i} t^{-s} \frac{\Gamma(s)\Gamma(b+s)\Gamma(\frac{1-b}{2} - s)}{\Gamma(\frac{1}{2} + b + s)} {}_2F_1\left(\frac{1}{2}, b; \frac{1}{2} + b + s; -1\right),$$

where $0 < d < (1-b)/2$. Closing the contour to the left, as we want a small t expansion, we see there are poles coming from the Gamma functions. The first occurs at $s = 0$, and the second at $s = -b$. Taking the residue at the poles we get

$$I(b, t) \approx \frac{\sqrt{\pi}\Gamma(b)}{2\Gamma(b + \frac{1}{2})} {}_2F_1\left(\frac{1}{2}, b; \frac{1}{2} + b; -1\right) - 2^{-b} c^b \frac{\Gamma(-b)\Gamma(\frac{1+b}{2})}{\Gamma(\frac{1-b}{2})}.$$

Another term comes from $I(b+1, t)$, and this gives a term

$$-b(\alpha-1) \frac{\sqrt{\pi}\Gamma(b)}{2\Gamma(b+\frac{1}{2})} {}_2F_1\left(\frac{1}{2}, 1+b; \frac{1}{2}+b; -1\right).$$

We can eliminate the hypergeometric functions, as they can be expressed in terms of Gamma functions, and then simplified. In this way we obtain

$$F(\alpha, b) \approx \frac{\sqrt{\pi}\Gamma(\frac{b}{2})}{\Gamma(\frac{b+1}{2})} + (\alpha-1)^b \cdot \frac{\Gamma(-b)\Gamma(\frac{1+b}{2})}{\Gamma(\frac{1-b}{2})} - (\alpha-1) \cdot \frac{b\sqrt{\pi}}{4} \left[\frac{\Gamma(\frac{b}{2})}{\Gamma(\frac{b+1}{2})} + \frac{\Gamma(\frac{b+1}{2})}{\Gamma(\frac{b}{2}+1)} \right].$$

We can write the ratio

$$\begin{aligned} \frac{N(\alpha, b)}{F(\alpha, b)} &= A \cdot c^b \cdot [1 + Bc + Dc^b + O(c^{2b})] = \\ &= A8^b e^{-b\pi r/2} \left(1 + D8^b e^{-b\pi r/2} + (4b + 8B)e^{-\pi r/2} + O(e^{-b\pi r}) \right). \end{aligned}$$

Here we have used the asymptotic expansion (3) of $\alpha-1$ as an expansion in α , and the parameters introduced above are

$$\Lambda = \frac{\Gamma(\frac{1+b}{2})^2}{\Gamma(\frac{b}{2})^2},$$

and

$$\begin{aligned} A &= \frac{\Lambda}{b \cdot 2^b}, \\ B &= -\frac{3b}{4} - \frac{1}{2} - \frac{\Lambda}{2}, \\ D &= \frac{\Lambda}{b \cdot 2^b \cdot \sin(\pi b/2)}. \end{aligned}$$

Then

$$\tilde{R}(r, b) = \frac{2^{2b+1}\Lambda}{b e^{b\pi r/2}} \left[1 + \frac{\Lambda 2^{2b+1} e^{-b\pi r/2}}{b \sin(\frac{\pi b}{2})} + 4(b-1+2\Lambda)e^{-\pi r/2} + O(e^{-b\pi r}) \right], \quad (8)$$

for $0 < b < 1$.

For $r = 10$ and $b = 5/8$ the leading term gives 4 significant digits accuracy (where we are comparing to the value obtained by numerical integration with 50 digit accuracy), while including the next terms gives 8 significant digits. This is more than sufficient for our purpose here. However for $r = 2$ (with the same value of b) the expansion is much more slowly convergent, and the above expression provides the result to an accuracy of merely 1 part in 20. While we could calculate further terms in the asymptotic expansion, we prefer to simply evaluate the integral expression (5) numerically.

We now use these results to calculate the value of b characterising the scaling limit of SAWs. We do this by generating all SAWs in a rectangle of given aspect ratio r , centred at the origin, and of size $2n \times 2rn$, for $n = 1, 2, \dots, n_{\max}$, where n_{\max} refers to the largest possible rectangle we can use given our computer resources.

In the next section we describe the efficient generation of these SAWs, using transfer matrices and efficient use of symmetry and the elimination of unnecessary starting points. In the following section we analyse the data thus produced, by calculating and extrapolating the ratio $R_n(r)$ for two representative values of r , which were $r = 2$ and $r = 10$. From these estimates of $R_\infty(r)$ we use the asymptotic expansion above to estimate b , in the case of aspect ratio 10, while for $r = 2$ the comparison is made with numerical integration values from (5).

Furthermore, we can compare the hitting density distribution function, as calculated from our largest rectangle, to that predicted in the scaling limit. With $b = 5/8$, and for rectangles of aspect ratio 2, it will be seen that the two distribution functions are almost indistinguishable.

2 Enumeration of SAWs hitting the short and long sides of the rectangle

We first describe the computation of the generating functions of a SAW starting at the centre of the strip and terminating, respectively, the first time it hits either one of the rectangle's two short sides, or one of its two long sides. The rectangle is supposed oriented so that the short sides are horizontal and the long sides vertical.

As usual in enumeration studies the basic ingredient is a transfer matrix acting on an appropriate set of states. Each state comes with a weight, which is a polynomial with integer coefficients in a variable x that is interpreted as the fugacity for one step of the SAW. The transfer matrix is maximally decomposed as a product of elementary matrices that each adds a small piece (a vertex and its adjacent half-edges) to the lattice being constructed. The states contain information about how the uppermost row of half-edges are connected among themselves, or to the boundary of the rectangle, or to the centre point, through pieces of the partially built SAW. This information—and the action of the elementary matrices on the states—must be carefully devised so that:

1. a single SAW going from the centre to the boundary of the rectangle is constructed;
2. the two desired generating functions, describing respectively the hitting of the short and long sides of the rectangle, can be disentangled;
3. no superfluous information is stored.

Points 1 and 2 are essential for the correctness of the algorithm, whereas 3 is only a matter of efficiency. It cannot be excluded that the precise procedure described below can be shown in the future not to be optimal, in the sense that a variant algorithm can be constructed that uses fewer states to achieve the goals 1 and 2.

We consider an $L \times W$ rectangle, with L and W even (so that the centre of the rectangle coincides with a vertex), and $L \leq W$ (the transfer matrix then propagates upwards). The states contain information about the connectivities of the n uppermost half-edges, labelled $0, 1, 2, \dots, n-1$ from left to right, of the partially constructed lattice. When a row of the lattice is completed, $n = L-1$ and all half-edges are vertical. At stages where a row is under construction, $n = L$ and one of the half-edges is horizontal. The lattice is constructed—through the action of the elementary matrices—row by row, completing the

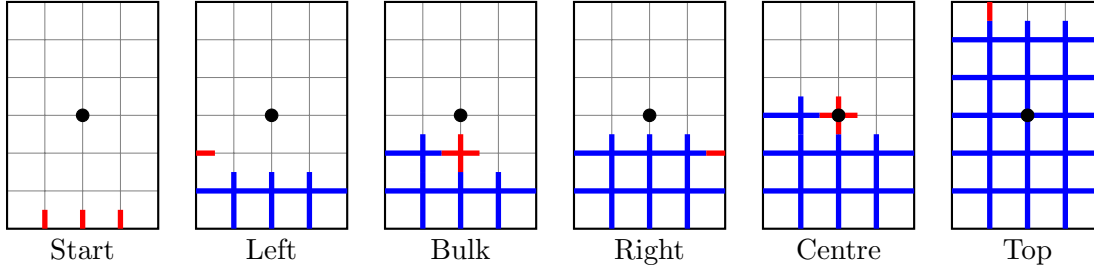


Figure 2: Various stages in the transfer matrix construction, here shown for a rectangle of size 4×6 . Each stage is labelled by a convenient name and will be explained fully in the main text. The parts of the lattice being constructed in any given stage is shown in red, while those already constructed in earlier stages are shown in blue. The black dot marks the centre of the rectangle.

rows from left to right. This is shown in Figure 2. Each half-edge can be connected to another half-edge, or be in one of the following configurations:

1. **EMPTY**, meaning that it is not covered by the SAW;
2. **SIDE**, when it is connected through the SAW to the left or right boundary of the rectangle;
3. **BOTTOM**, when its is connected to the bottom (or top) boundary of the rectangle;
4. **CENTRE**, when it is connected to the centre point.

In addition the system as a whole can be in the following configurations when the SAW has been completed before the lattice has been completely built:

5. **EXIT_LR** when the SAW went from the centre point to the left or right boundary;
6. **EXIT_BT** when it went to the bottom or top boundary.

Being in one of those exit configurations implies that all the half-edges must be empty and remain so until completion of the lattice. To describe such states it is therefore sufficient to use just $n = 1$ label containing the exit status (**EXIT_LR** or **EXIT_BT**).

Imposing the correct constraints throughout the construction of the lattice (see below) will imply that once the lattice has been completed only the two exit states carry a non-zero weight. These two weights are precisely the desired generating functions.

We now describe the action on the states of the different elementary matrices that build up the system (see Figure 2).

In the initial stage, called **Start** in Figure 2, the system is in a superposition of the completely empty state (with weight 1), and each of the n states where one of the $n = L - 1$ half-edges carries the **BOTTOM** label (with weight x) and the others are **EMPTY**. Note that a valid state cannot have more than one half-edge labelled either **BOTTOM** or **SIDE**, since we aim at constructing a SAW that touches the boundary in only one single point.

After a row of the lattice has been completed the following operation, called **Left** in Figure 2, adds a horizontal half-edge touching the left boundary of the rectangle. If the system is already in an exit state it remains so and with the same weight. Otherwise the labels are shifted one unit to the right to make place for that of the horizontal half-edge. The latter can either be **EMPTY** or, if no other **BOTTOM** or **SIDE** label exists, be set to **SIDE** in which case the weight is multiplied by x to take account for the extra monomer.

The subsequent operations within the row are of the type **Bulk**. The elementary matrix now acts on two labels, describing the half-edges coming from West and South in the incoming state, and which after the time evolution describe the half-edges going towards North and East in the outgoing state. An exit state is treated as before. In all other cases we must ensure that the bulk vertex is adjacent to either two or four occupied edges. Thus, if both incoming labels are **EMPTY**, the outgoing labels can be **EMPTY** as well, or mutually connected with an extra weight x^2 . If only one incoming label is **EMPTY**, the other can go straight through the vertex or make a turn, in both cases with weight x . Finally, if neither of the incoming labels is **EMPTY** there is a rather large number of possibilities:

1. If both labels describe connectivities to other half-edges (i.e., neither is equal to one of the special labels **EMPTY**, **SIDE**, **BOTTOM** or **CENTRE** described above), their respective partner half-edges must be mutually connected. However, if the connection is among the two incoming half-edges themselves, the state must be discarded, since the SAW is not allowed to form a closed loop.
2. If one of the labels is special, the partner of the non-special label becomes equal to the special label.
3. Finally, if both incoming labels are special, we have the opportunity of creating an exit state. But first a number of precautions must be taken:
 - (a) All the remaining labels in the state need to be **EMPTY**, otherwise the state must be discarded.
 - (b) One of the incoming labels must be **CENTRE** and the other either **SIDE** or **BOTTOM** (otherwise discard the state). The latter label then determines whether the exit state is **EXIT_LR** or **EXIT_BT**.

In all those cases the two outgoing labels will be **EMPTY** and the weight coincides with that of the incoming state.

To complete a row we use the operation **Right**. The elementary matrix acts on the rightmost label, describing the half-edge that will touch the right boundary of the rectangle. The action on exit states is as usual. If the incoming label is **EMPTY** the state is kept as it is. Otherwise the rightmost half-edge will be occupied, and we must first make sure that there is not already a label which is **SIDE** or **BOTTOM** (otherwise discard the state). Next, if the incoming label is **CENTRE** we obtain an **EXIT_LR** exit state provided that the remainder of the half-edges are empty. Otherwise, if the incoming half-edge is connected to another half-edge, the latter will be marked by a **SIDE** label to signify the hitting of the right boundary of the rectangle. After these considerations the rightmost label is deleted, since we have now completed a row of the lattice and only $L - 1$ labels are required.

Special care must be taken when attaining the centre point. This is achieved by applying the operation **Centre**. As in the **Bulk** case the action is on two labels, but while in the former case the vertex had degree two or four, the number of occupied adjacent edges must now be one, since the SAW emanates from the centre point. Thus, if both incoming labels are **EMPTY** we produce two outgoing states with one of the outgoing labels being **CENTRE** and the other **EMPTY** (with a weight x). States with two occupied ingoing labels must be discarded. And finally, for states with one ingoing label being **EMPTY** and the other occupied there are a number of possibilities:

1. If the occupied incoming half-edge is connected to another half-edge, the latter acquires the **CENTRE** label.
2. Otherwise the occupied incoming half-edge is of the type **SIDE** or **BOTTOM**, and we end up in an exit state (provided the remainder of the system is empty).

It remains to describe how to finish the rectangle after building the last row. Each half-edge must now be subjected to the operation **Top** in order to implement the top boundary of the rectangle. The corresponding elementary matrix acts on a single label (and is in fact very similar to the operation **Right** described above). If that label is **EMPTY** the state is unchanged. If it is **SIDE** or **BOTTOM** the state is discarded. If it is connected to another half-edge, the latter acquires the **BOTTOM** label (which is ill-named in this case, since it is the top boundary of the rectangle which is being touched). And finally, if the incoming label is **CENTRE** we end up in the **EXIT_BT** state (provided the remainder of the system is empty).

From a practical point of view, all the labels used to describe a state can be coded on short integers (say, of the **char** type in **C**) and the coding of the entire state of n half-edges is then an array of characters. The handling of incoming and outgoing states is then conveniently and efficiently done by employing standard hashing techniques. The integer coefficients entering the weights will obviously become very large for even a moderately-sized system, but this is easily dealt with by using modular arithmetic, i.e., repeating the entire computation modulo various primes and reconstituting the results from the Chinese remainder theorem.

Our results for the generating functions with various aspect ratios are so lengthy that it makes little sense to have all them all appear in print. However, the complete results are available in electronic form as supplementary material to this paper.¹ For the convenience of the readers who wish to check explicitly the example of the 4×6 rectangle shown in Figure 2 we give the results for that case. For the hitting of the long sides of the rectangle we find

$$2x^2 + 8x^3 + 16x^4 + 12x^5 + 32x^6 + 28x^7 + 52x^8 + 40x^9 + 76x^{10} + 56x^{11} + 116x^{12} + 60x^{13} + 68x^{14}, \quad (9)$$

while for the hitting of the short sides we have

$$2x^3 + 12x^4 + 12x^5 + 24x^6 + 12x^7 + 32x^8 + 20x^9 + 60x^{10} + 44x^{11} + 100x^{12} + 28x^{13} + 56x^{14}. \quad (10)$$

¹This text file provided (named **GJ13.m**) can be processed by **MATHEMATICA** or—maybe after minor changes of formatting—by any symbolic computer algebra program of the reader's liking.

L	N_1	N'_1	N_2	N'_2
4	28	18	38	25
6	162	102	332	211
8	1 038	646	2 844	1 779
10	7 082	4 376	24 248	15 031
12	50 448	31 022	206 978	127 557
14	370 866	227 268	1 772 136	1 087 711
16	2 792 724	1 706 934	15 225 302	9 317 161
18	21 431 970	13 072 764		80 130 487

Table 1: Maximum number of states in the transfer matrix algorithm for an $L \times W$ rectangle with $W \geq L$. Here N_1 (resp. N_2) refers to the time evolution before (resp. after) the addition of the centre point. The corresponding primed quantities, N'_1 and N'_2 , are for the improved algorithm that exploits reflection symmetries.

Note that all the coefficients in this example are even. This is generally true and due to the symmetries of the rectangle. Explicitly, the mirror symmetry with respect to a horizontal (resp. vertical) line going through the centre point induces a bijection between the SAWs that hit the bottom (resp. left) boundary and those that hit the top (resp. right) boundary.

We can take advantage of those symmetries to make a more efficient version of the algorithm. Namely, if we impose the restriction that all the half-edges incident on the bottom and left boundaries be empty, only the SAWs hitting the right and top boundaries will be counted. This means that the required generating functions are simply divided by a factor of two. The reason that we have imposed the constraint on the left boundary rather than the right, and on the bottom boundary rather than the top, is that the left and bottom boundaries are those encountered earliest in the time evolution of Figure 2. Imposing the constraints early on will most efficiently curb the proliferation of unnecessary states.

It is quite simple to implement these changes. To keep the bottom boundary empty, it suffices to modify the stage **Start** so that initially the system is simply in the completely empty state (with weight 1). To keep the left boundary empty, we modify the **Left** operation so that the leftmost half-edge cannot acquire the **SIDE** label. The maximum number of states encountered in the time evolution are compared in Table 1 for the original and the improved algorithms. It is seen that the improvement diminishes the number of states by a factor that is asymptotically $\simeq 1.65$.

3 Full hitting distribution

We have also developed a refined enumeration scheme in which the full hitting distribution is recorded. The relevant geometry is shown in Figure 3. We wish to obtain separately the generating functions for SAWs starting at the centre of the rectangle and exiting at any prescribed point on its boundary. Due to the reflection symmetries it is enough to consider exits on the right and top boundaries. Each exit point on the right (resp. top) boundary can be labelled by its vertical (resp. horizontal) coordinate c_y (resp. c_x) with respect to

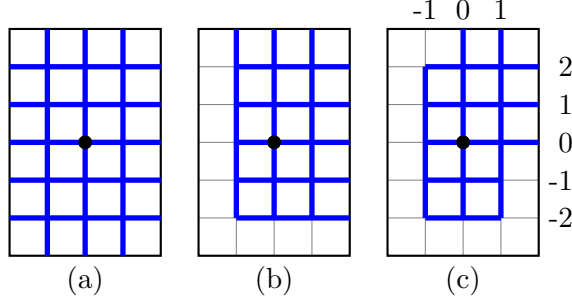


Figure 3: Boundary conditions that exploit the reflection symmetries of the lattice and improve the efficiency of the computations. The full lattice (a) can be reduced by depleting its bottom and left boundaries (b), and further depleting one half of the right and top boundaries (c). The coordinate c_x (resp. c_y) labelling the horizontal (resp. vertical) exit point is defined in panel (c).

the centre of the rectangle, as shown in Fig. 3c. Again invoking the reflection symmetries, the generating functions only depend on $|c_x|$ and $|c_y|$, so it is enough to consider the cases $c_x \geq 0$ and $c_y \geq 0$. Therefore the full lattice (Fig. 3a) can effectively be replaced, first by a lattice with empty bottom and left boundaries (Fig. 3b), and next by a lattice with half of the top and right boundaries empty as well (Fig. 3c).

The changes to the original program when going from the lattice shown in Fig. 3b to that in Fig. 3c are completely analogous to those described in the preceding section when going from the lattice shown in Fig. 3a to that in Fig. 3b.

The only other change required to obtain the full hitting statistics is to register the coordinate (c_x or c_y) of the exit point. This is done by including one extra integer in the characterisation of each state. This integer, initially set to zero, is unchanged in most of the evolution process, except at the unique stage where an occupied monomer hits the boundary. At that stage it is set to the coordinate value of the exit point. To be precise, this happens either when a **SIDE** or **BOTTOM** label is attached to the state, or when then **CENTRE** label hits the boundary.

The results for our usual example of the $L \times W = 4 \times 6$ rectangle are as follows:

$$\begin{aligned}
 c_x = 0 & : x^3 + 6x^5 + 6x^7 + 10x^9 + 22x^{11} + 14x^{13} \\
 c_x = 1 & : 3x^4 + 6x^6 + 8x^8 + 15x^{10} + 25x^{12} + 14x^{14} \\
 c_y = 0 & : x^2 + 2x^4 + 4x^6 + 10x^8 + 8x^{10} + 8x^{12} + 6x^{14} \\
 c_y = 1 & : 2x^3 + 3x^5 + 7x^7 + 10x^9 + 14x^{11} + 15x^{13} \\
 c_y = 2 & : 3x^4 + 6x^6 + 8x^8 + 15x^{10} + 25x^{12} + 14x^{14}
 \end{aligned} \tag{11}$$

Summing over c_y , and multiplying by two to take into account both the left and the right boundaries, we recover (9). Similarly, summing over c_x we recover (10). Another general feature brought out by (11) is that all powers of x within a given generating function must have the same parity. This parity can be inferred from the length of the shortest SAW to the relevant boundary, i.e., it is the same parity as that of $\frac{W}{2} + c_x$ (resp. $\frac{L}{2} + c_y$).

L	N_1''	N_2''
4	8	49
6	42	665
8	254	7 879
10	1 670	86 165
12	11 596	898 727
14	83 670	9 097 463

Table 2: Maximum number of states in the full hitting statistics algorithm for an $L \times W$ rectangle with $W = 2L$. Here N_1'' (resp. N_2'') refers to the time evolution before (resp. after) the addition of the centre point. These numbers should be compared with those in Table 1.

Finally, we remark that a SAW attaining the internal vertex v_{int} closest to the upper right corner of the rectangle must necessarily exit at one of the two neighbouring vertices on the boundary, i.e., contribute either to the generating function with $c_x = L/2 - 1$ or the one with $c_y = W/2 - 1$. Conversely, any SAW hitting one of these two boundary points must necessarily pass through v_{int} . The two generating functions are thus equal, and this general result is of course brought out by (11).

The need to register the exit coordinate obviously increases the number of states used in the computation. One might expect that roughly $W/2$ times more states would be needed. Fortunately, the additional constraints imposed on the boundary half-edges ameliorates the situation somewhat. The maximum number of states needed by the full hitting statistics algorithm are shown in Table 2.

4 Analysis of data

In Table 3 we give the ratio $R_n(2)$ of the number of walks hitting the long side to that of the number of walks hitting the short side for a rectangle with aspect ratio 2.

Table 3: Ratio of number of walks first hitting long side to the number hitting the short side for a $n \times 2n$ rectangle, $R_n(2)$.

n	Ratio $R_n(2)$
2	4.6381585303417408684303075667444130488805022010318359737078706077696
4	4.5626403997998714832892051885980313566654043362375413463572606810903
6	4.5737694425659079263885691980864259391038701844156223313634364418527
8	4.5816876116611105157124235041836861179217970948263182063453368731855
10	4.586835597801674598789736657813550866717170851432063193366000200424
12	4.590372957831729906013721282115051244422423169272971142266883828004
14	4.592938409379941423415363287957199443993269739941033366762062737428
16	4.594881296788588474819955070086767540896832163815763639405593859180
18	4.5964037339238675392443305096632781995673848727512239850106566816295

This has been calculated by evaluating the ratio of the two “generating functions”

(which are of course polynomials, as we are dealing with finite lattices) at x_c . For the square lattice x_c is not exactly known, but the best numerical estimate, $x_c = 0.37905227774965(13)$ [5], is in agreement with the mnemonic $581x^4 + 7x^2 - 13 = 0$ [6], and it is the appropriate root of this polynomial equation that we are using. Our results are insensitive to the uncertainty in the best numerical estimate of x_c .

This ratio is seen to be monotonically decreasing, and a plot of the data suggests behaviour of the form $R_n(r) \sim c + d/n^\theta$. In order to estimate θ , we notice that a log-log plot of n against $R_n(2) - R_{n-1}(2)$ has gradient -2.0 ± 0.08 . This implies $\theta = 1 \pm 0.08$, and in our subsequent analysis we assume $\theta = 1$. We then extrapolated the sequence $\{R_n(2)\}$ by the Bulirsch-Stoer algorithm [20], with the free parameter in that algorithm set to reflect $\theta = 1$. The analysis is shown in Table 4.

Table 4: Extrapolation of the data in Table 3 by the Bulirsch-Stoer algorithm

4.589060	4.694672	4.609872	4.608214	4.608850	4.609984	4.609630
4.600917	4.615954	4.608989	4.608787	4.608949	4.609718	
4.604615	4.611393	4.608899	4.609077	4.608726		
4.606178	4.610139	4.608975	4.609228			
4.606991	4.609677	4.609086				
4.607480	4.609489					
4.607806						

In this way we estimate the limiting ratio as 4.6096 ± 0.0002 .

We also analysed the data by several other appropriate extrapolation algorithms. The Brezinski θ algorithm [9] gives an increasing sequence of estimates for the large n limit of the ratios, suggesting that the limit $\lim_{n \rightarrow \infty} R_n(2) > 4.6094$. Levin's u -transform [9] gives a monotone decreasing sequence of estimates, suggesting that $\lim_{n \rightarrow \infty} R_n(2) < 4.6097$. Neville tables [9] also give a monotone increasing sequence of estimates, suggesting that $\lim_{n \rightarrow \infty} R_n(2) > 4.6090$. These are all consistent with our estimate from the Bulirsch-Stoer algorithm. This gives $b = 0.62501 \pm 0.00003$, or $\kappa = 2.66664 \pm 0.00007$.

In Table 5 we give the corresponding, slightly shorter data set, for walks in a rectangle of aspect ratio 10. By a similar analysis, we estimate the limit to be $R_n(10) = 14955 \pm 15$. From (8) this implies $b = 0.62496 \pm 0.000066$, or $\kappa = 2.66675 \pm 0.00015$.

Table 5: Ratio of number of walks first hitting the long side to the number hitting the short side for an $n \times 10n$ rectangle, $R_n(10)$.

n	Ratio $R_n(10)$
4	14006.18549331435655361766127203880086492399593549150863381964074817
6	14245.30058306730412888413593536062491411218703615652940541335814143
8	14391.29165062927743781254092745976155303961361728983232311816771246
10	14487.00740644606426682399787816797507371639547391783093463818418043
12	14554.35495421800301499956345001503940598563417509710466751030105068
14	14604.3566053623407864953033765640802317538963314516614175885263116878

As well as calculating the ratio of the number of walks hitting the long side to that of

the number of walks hitting the short side of a rectangle with aspect ratio 2, we have also calculated the distribution of hitting densities along the long side of such a rectangle. For the case of a 14×28 rectangle, the data is shown in Table 6. From (2) it follows that the (unnormalized) probability density satisfies

$$\rho_{f(D)}(f(z)) \propto \rho_D(z)|f'(z)|^{-b},$$

where

$$f'(z) = (1 - z^2)^{-1/2}(\alpha^2 - z^2)^{-1/2}$$

follows from the Schwarz-Christoffel transformation previously discussed, and the unrenormalized hitting density along the real axis is $(z^2 + \alpha)^{-b}$, as follows from (1)–(2), and is described in detail in [11]. So the hitting density along the long side of the rectangle is (up to a multiplicative constant),

$$(z^2 + \alpha)^{-b}(1 - z^2)^{b/2}(\alpha^2 - z^2)^{b/2},$$

where the corresponding ordinates follow from the Schwarz-Christoffel transformation, so that the ordinates $(0, 1/14, \dots, 13/14)$ transform as

$$n/14 \rightarrow \int_0^{n/14} \frac{1}{\sqrt{1-t^2}} \frac{dt}{\sqrt{\alpha^2-t^2}} = \frac{1}{\alpha} \mathbf{F}\left(\frac{n}{14}, \frac{1}{\alpha}\right),$$

where \mathbf{F} is the incomplete elliptic integral of the first kind. In figure 4 we show the predicted hitting density data for a rectangle of aspect ratio 2 together with the measured data for SAWs in a 14×28 rectangle. The enumeration data has been scaled linearly to make the origin and end-points coincide. Despite the fact that a 14×28 rectangle would seem to be rather far from the scaling limit, the agreement is remarkably good.

5 Conclusion

We first calculated the ratio of the number of SAWs starting at the centre of a rectangle and hitting the end to that of the number of SAWs starting at the centre of a rectangle and hitting the sides, for rectangles of a given aspect ratio. Then by comparing this to the calculated value [11] assuming that the scaling limit of SAWs is given by SLE_κ , we estimated κ for rectangles of aspect ratio 2 and 10. In the former case we found $\kappa = 2.66664 \pm 0.00007$, and in the latter case we found $\kappa = 2.66675 \pm 0.00015$. This would appear to be the strongest numerical support yet for the widely held belief that the scaling limit of SAWs is given by $SLE_{8/3}$.

Furthermore, we have also calculated the distribution of hitting densities along the long side of such a rectangle and compared this with the actual distribution for a 14×28 rectangle. Visually, the agreement between the plots of the two distributions is seen to be quite persuasive.

Table 6: Hitting distribution for a 14×28 rectangle. The third column gives the (unnormalized) fraction of walks hitting the long boundary at $\pm n/14$, where n is given in column 1 and $n/14$ in column 2.

n	$n/14$	Hitting number
0	0.000000000000000000000000000000	0.372179965985066951892060536379
1	0.071428571428571428571428571428	0.365592202518487166323769503648
2	0.142857142857142857142857142857	0.347584595139263204799699150831
3	0.214285714285714285714285714286	0.321757459504506388412145573956
4	0.285714285714285714285714285714	0.291774774902074605895271622535
5	0.357142857142857142857142857143	0.260478252386315460357350977416
6	0.428571428571428571428571428571	0.229709762715325246279406382177
7	0.500000000000000000000000000000	0.200461104152704918984187699069
8	0.571428571428571428571428571429	0.173099730010024355136783990185
9	0.642857142857142857142857142857	0.147556785152232511539056308909
10	0.714285714285714285714285714286	0.123439559572782004646612438472
11	0.785714285714285714285714285714	0.100052601022725874927123950740
12	0.857142857142857142857142857143	0.076292442893068500584108376384
13	0.928571428571428571428571428571	0.050321628007048540057861695734

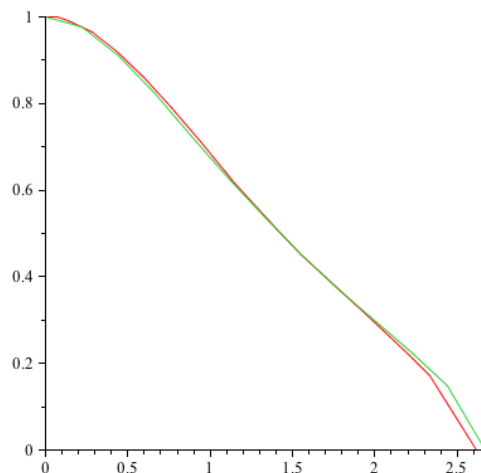


Figure 4: Hitting density distribution function for a 12×24 rectangle (green) compared to the theoretical prediction in the scaling limit with $b = 5/8$ (red).

Acknowledgements

This work was supported by the Australian Research Council through grant DP120100939 (AJG and JLJ), and by the Institut Universitaire de France and Agence Nationale de la Recherche through grant ANR-10-BLAN-0414 (JLJ). AJG would like to thank Larry

Glasser for a lesson in asymptotic expansions, Tom Kennedy for a lesson in conformal mapping, and both authors would like to gratefully acknowledge the support of the Simons Center for Geometry and Physics at SUNY Stony Brook where this work was, in part, carried out.

References

- [1] Beffara V (2010) Schramm-Loewner Evolution and other conformally invariant objects, Clay Mathematics Institute Summer School, Buzios
- [2] Bornemann F, Laurie D, Wagon S and Waldvogel J (2004), *The Siam 100-Digit Challenge: A study in high-accuracy Numerical Computing*, SIAM Philadelphia
- [3] Borwein J (2005), *Mathematical Intelligencer* **27**, 40-48
- [4] Clisby N (2010), Efficient implementation of the pivot algorithm for self-avoiding walks, arXiv:1005.1444, *J. Stat. Phys.* **140** 349–392
- [5] Clisby N and Jensen I (2011), A new transfer-matrix algorithm for exact enumerations: Self-avoiding polygons on the square lattice, arXiv:1111.5877v1
- [6] Conway A R, Enting I G and Guttmann A J (1993), Algebraic techniques for enumerating selfavoiding walks on the square lattice, *J. Phys. A:Math. Gen* **26** 1519–34.
- [7] Dyhr B, Gilbert M, Kennedy T, Lawler G and Passon S (2011) The self-avoiding walk spanning a strip, *J Stat Phys.* **144** 1–22
- [8] Enting I G and Jensen I (2009) in *Polygons, Polyominoes and Polycubes*, Lecture Notes in Physics **775**, Guttmann A J (ed.), Springer (The Netherlands)
- [9] Guttmann A J (1989) in *Phase Transitions and Critical Phenomena, vol 13*, eds. Domb C and Lebowitz J, Academic Press, London and New York.
- [10] Guttmann A J (ed.) (2009) *Polygons, Polyominoes and Polycubes*, Lecture Notes in Physics **775**, Springer (The Netherlands)
- [11] Guttmann A J and Kennedy T (2013) Self-avoiding walks in a rectangle, arXiv:1210.7924 To appear in *J. Eng. Math.*
- [12] Kennedy T (2001) Monte Carlo tests of SLE predictions for the 2D self-avoiding walk. *Phys Rev Lett.* **88**, 130601
- [13] Kennedy T (2012) Simulating self-avoiding walks in bounded domains, *J. Math. Phys.* **53**, 095219
- [14] Kennedy T and Lawler G F (2011) Lattice effects in the scaling limit of the two-dimensional self-avoiding walk, arXiv:1109.3091v1
- [15] Lawler G, Schramm O and Werner W (2004) On the scaling limit of planar self-avoiding walk, *Fractal Geometry and Applications: a Jubilee of Benoit Mandelbrot, Part 2*, 339-364, Proc. Sympos. Pure Math. 72, Amer. Math. Soc., Providence, RI (arXiv:math/0204277v2)

- [16] Löwner K (1923) Untersuchungen über schlichte konforme Abbildungen des Einheitskreises. I. Math. Ann. **89**, 103–121
- [17] Madras M and Slade G (1993) The self-avoiding walk, Probability and its Applications. Birkhäuser Boston Inc., Boston, MA
- [18] Petrović V V (2009) Comprehensive table of Singular Moduli, http://mtt.etf.ac.rs/Singular_Moduli_www/SingularModuliVVP.pdf
- [19] Riesz F and M (1916) Über die Randwerte einer analytischen Funktion, Quatrième Congrès des Mathématiciens Scandinaves, Stockholm, pp 27-44
- [20] Stoer J and Bulirsch R (1980) *Introduction to Numerical Analysis*, Springer-Verlag
- [21] Trefethen LN (2002) SIAM News, **35**, No. 1 Jan/Feb. Also (2002) SIAM News, **35**, No. 6, July/Aug.